Heteroclinic Chaos in Attitude Dynamics of a Dual-Spin Spacecraft at Small Oscillations of Its Magnetic Moment

ANTON V. DOROSHIN

Space Engineering Department (Division of Flight Dynamics and Control Systems)
Samara State Aerospace University (SSAU)
SSAU, Moscowskoe shosse 34, Samara, Russia 443086
doran@inbox.ru

Abstract: - The paper contains an investigation results in the heteroclinic dynamics of a magnetic (magnetized) dual-spin spacecraft (DSSC) in the geomagnetic field at the realization of the orbital motion of its mass centre along an equatorial circular orbit. Exact heteroclinic analytical solutions are obtained. These analytical exact solutions are used for the research of the DSSC perturbed motion and its chaotization properties at the presence of small polyharmonic perturbations of the magnetic moment.

Key-Words: - Magnetic/Magnetized Dual-Spin Spacecraft; Heteroclinic Explicit Solutions; Melnikov Function; Lagrange Top; Euler Top; Chaos

1. Introduction

Chaotic regimes in the angular/attitude motion of multibody systems/spacecraft and the corresponding many-sided research's aspects are undoubtedly very important parts of modern non-linear mechanics, including spaceflight dynamics [1-42].

One of the main multibody spacecraft's schemes is the dual-spin spacecraft (DSSC) which represents the mechanical system of coaxial bodies and the single-rotor gyrostat. The versatile explorations of the DSSC/gyrostat's dynamics were conducted in many research works devoted in different formulations to the analytical/numerical modeling of unperturbed/perturbed modes and to obtaining of exact/approximate solutions for the motion under influence of different external/internal disturbances (gravity, aerodynamic torques, dissipative/excitative effects from external environments, interactions between the system bodies, etc.) [e.g. 5-31].

Equally with numerous types of perturbations acting on the DSSC, the (electro)magnetic torque from the Earth's magnetic field is the very important dynamical factor. It is needed to note that numerous works and publications were connected with the investigation of the attitude dynamics/control of the magnetic (magnetized) spacecraft, for example [32-42]. Here we can underline the connection of the task of the attitude motion of the magnetized DSSC with classical tasks of the rigid body mechanics (the Euler, the Lagrange tops) [1-4].

The "magnetic" torque arises due to DSSC usually contains internal electrical equipment with powerful inductive elements and magnets. Also this factor can be one of the main reasons of the chaos initiation in the DSSC dynamics. The consideration of connected causes and effects of the heteroclinic chaotization is the primary task of this paper.

So, in this paper the chaotization analysis of the attitude dynamics of the magnetic/magnetized DSSC is provided. This analysis is based on the Melnikov function evaluation along heteroclinic trajectories in the phase space of the magnetic/magnetized DSSC, which performs an orbital motion on a circular equatorial orbit at the realization of the spin-stabilized attitude motion in the "cylindrical precession" regime, when the angular momentum of the DSSC is directed perpendicularly to the orbit's plane. This motion regime is quite important for the practice because it corresponds (in ideal conditions) to one of the preferred regimes of the stationary attitude motions of the DSSC with the conservation of the spatial orientation of its longitudinal axes (especially it is important for communication satellites).

The paper material is presented the continuation and expansion of the previous author's analytical research [26] into the applied aria corresponding to the magnetic DSSC chaotic motion investigation. The main paper results connected with obtaining of analytical heteroclinic solutions and with the illustration of non-regular regimes of the motion dynamics. Also the paper results can be additionally investigated in aspects of non-trivial complex dynamical modes implementation with the help of modern simulation tools [43-49].

2. Equations of the attitude dynamics of the magnetic/magnetized DSSC

Let us by analogy with [26] consider the attitude dynamics of the DSSC which contains the internal permanent magnet or the inductive elements (current-carrying inductive coils) with the magnetic dipole moment **m** under the influence of the external magnetic field (and with corresponding magnetic restoring/overturning torque $\mathbf{M_\theta}$). Assume that the mass centre of the DSSC is moved along the circular equatorial orbit of a planet (e.g. the Earth) which has the ideal single dipole magnetic field. In conditions of the DSSC orbital motion on circular equatorial orbit we can consider the planet's magnetic field vector $\mathbf{B_{orb}}$ as constant vector (Fig.1) which is orthogonal to the orbit plane ($\mathbf{B_{orb}}$ is the tangent vector to the surface of the magnetic field (Fig.1)); the magnitude of this vector depends on the altitude of the circle equatorial orbit.

The DSSC usually consist from two coaxial bodies (body #1 is a rotor; body #2 is a main/core/carrier body). The rotor-body rotates in the inertial space with an angular velocity $\boldsymbol{\omega_1}$, and the main carrier body rotates with an angular velocity $\boldsymbol{\omega_2}$. The angular velocity of the rotor-body differs from the angular velocity of the main carrier body on a vector of a relative rotation angular velocity $\boldsymbol{\sigma}$ about a common longitudinal DSSC axes ($\boldsymbol{\omega_1 = \omega_2 + \sigma}$).

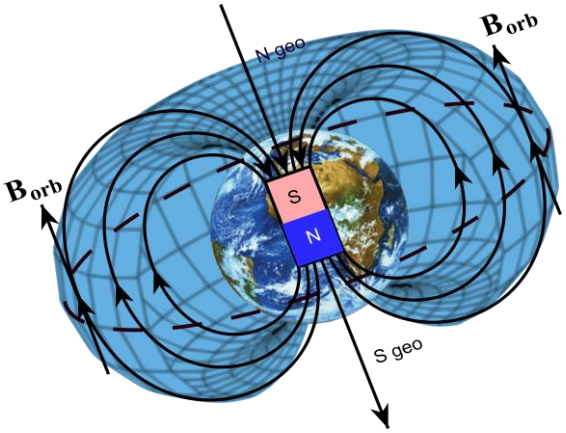

Fig.1 *The ideal single dipole model of the Earth's magnetic field, and the constant magnetic field vector* $\mathbf{B_{orb}}$ *corresponding to the circle equatorial orbit*

We will use the following frames (Fig.2-a): *OXYZ* is the main inertial ("fixed") system of coordinates with origin *O* in the mass centre of the DSSC, where the axis *OZ* is collinear with the constant magnetic vector of the external magnetic field (**k'** is the unit vector of the *OZ* axis) and then $\mathbf{B_{orb}} = B_{orb}\mathbf{k'}$; $Ox_2y_2z_2$ is the connected principal system of coordinates of the carrier body (**i**, **j**, **k** are the corresponding unit vectors); and $Ox_1y_1z_1$ – the connected principal system of coordinates of the rotor body.

The axes Oz_1 and Oz_2 of the connected systems coincide with the common longitudinal axis of the DSSC's coaxial bodies. We assume that the main body has a triaxial inertia tensor, and the rotor is a body with the dynamical symmetry (the equatorial inertia moments are equal).

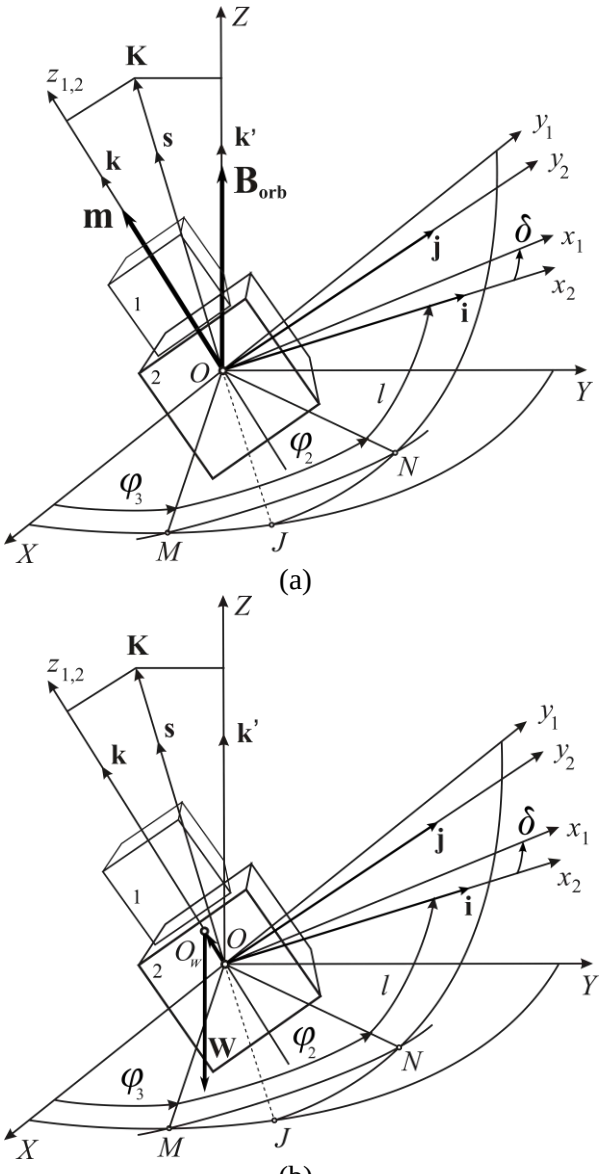

Fig.2 *Frames of the magnetic/magnetized DSSC's (a) and the corresponding analogy with the "heavy coaxial top" (b)*

Moreover, we consider the case (Fig.2-a) when

the DSSC's intrinsic magnetic moment is aligned with the DSSC's longitudinal axis $\left(\mathbf{m} = m\mathbf{k}\right)$.

The Euler general dynamical equations of the system can be written with the help of the low of the angular momentum changing in the rotating with the angular velocity $\boldsymbol{\omega}_2$ frame $Ox_2y_2z_2$

$$\dot{\mathbf{K}} + \boldsymbol{\omega}_2 \times \mathbf{K} = \mathbf{M}^{\mathbf{e}} \tag{1}$$

where $\mathbf{K}$ is the system angular momentum, $\mathbf{M}^{\mathbf{e}}$ – is the vector of external torques.

The scalar form of the vector equation (1) represents the following system:

$$\begin{cases} A\dot{p} + \left(C - B\right)qr + qC_1\sigma = M_x^e \\ B\dot{q} + \left(A - C\right)pr - pC_1\sigma = M_y^e \\ C\dot{r} + C_1\dot{\sigma} + \left(B - A\right)pq = M_z^e \\ C_1\left(\dot{r} + \dot{\sigma}\right) = \dot{\Delta} = M_\Delta \end{cases} \tag{2}$$

where $\left\{p, q, r\right\}$ are the components of the carrier body's angular velocity $\boldsymbol{\omega}_2$ in projections onto the axes of the $Ox_2y_2z_2$ frame; σ is the rotor angular velocity relatively the carrier body $\left(\sigma = \dot{\delta}\right)$; $\mathbf{I}_2 = diag\left[A_2, B_2, C_2\right]$ is the triaxial inertia tensor of the carrier body in the connected frame $Ox_2y_2z_2$; $\mathbf{I}_1 = diag\left[A_1, A_1, C_1\right]$ is the inertia tensor of the dynamically symmetrical rotor in the connected frame $Ox_1y_1z_1$; $A = A_1 + A_2$, $B = A_1 + B_2$, $C = C_1 + C_2$ are the main inertia moments of the coaxial bodies system in the frame $Ox_2y_2z_2$ (including rotor); $\Delta = C_1\left(r + \sigma\right)$ – the longitudinal angular moment of the rotor along Oz_1; $C_1\sigma = h_{z_1}$ – the rotor relative angular moment in the carrier body frame $Ox_2y_2z_2$. M_Δ – is the internal torque of the coaxial bodies interaction. Let us consider the following mass-inertia distribution $A > B > C$.

We ought to note that the orbital motion of the spacecraft can be considered as the motion fulfilled under the action of such perturbations as the magnetic torque, the gravity gradient torque, the small aerodynamics drag from the Earth's atmosphere, and other disturbances (the solar pressure torque, etc.). These perturbations have magnitudes, which can essentially differ from each other.

The torque of the magnetic interaction of the magnetic/magnetized DSSC with the external magnetic field is

$$\mathbf{M}_{\boldsymbol{\theta}} = \mathbf{m} \times \mathbf{B}_{\mathbf{orb}};$$

$$\mathbf{M}_{\boldsymbol{\theta}}\big|_{Ox_2y_2z_2} = \left[M_{\theta x}, M_{\theta y}, M_{\theta z}\right]^T = \tag{3}$$

$$= B_{orb}m\left[-\gamma_2, \gamma_1, 0\right]^T;\ B_{orb} = \frac{\mu_0\mu_m}{4\pi R^3}$$

Here μ_0 is the magnetic permeability of free space $\left(\mu_0 = 4\pi \cdot 10^{-7}\left[\mathrm{T \cdot m/A}\right]\right)$; $\mu_m \approx 7.8 \cdot 10^{22}$ [A·m^2] is the geomagnetic dipole moment; R is the orbit's altitude (relative the mass centre of the Earth); m is the magnetic moment of the DSSC (m~100÷1000 [A·m^2] – it corresponds, e.g., to the magnet of the ordinal system of the SC angular momentum shedding); parameters γ_i are the directional cosines of the axis OZ (the "fixed" inertial direction of the $\mathbf{B}_{\mathbf{orb}}$ vector) in the main body frame $Ox_2y_2z_2$:

$$\begin{aligned} \gamma_1 &= \mathbf{i} \cdot \mathbf{k}' = \cos\left(OZ, Ox_2\right), \\ \gamma_2 &= \mathbf{j} \cdot \mathbf{k}' = \cos\left(OZ, Oy_2\right), \\ \gamma_3 &= \mathbf{k} \cdot \mathbf{k}' = \cos\left(OZ, Oz_2\right) \end{aligned} \tag{4}$$

The torque corresponding to the gravity gradient can be written in the form

$$\mathbf{M}_G\big|_{Ox_2y_2z_2} = \left[M_{Gx}, M_{Gy}, M_{Gz}\right]^T =$$

$$= \frac{3\mu_G}{R^3}\delta_I\left[\frac{C - B}{\delta_I}\beta_2\beta_3, \frac{A - C}{\delta_I}\beta_3\beta_1, \frac{B - A}{\delta_I}\beta_1\beta_2\right]^T,$$

where $\mu_G = Gm_e = 3.986 \cdot 10^{14}$ N·m^2/kg is the Earth's mass-gravity parameter; β_i are the directional cosines of the axis of the local normal to the circular orbit of the DSSC (the local direction to the gravity centre); and $\delta_I = A - C$ is the difference between the largest and the smallest inertia moment of the DSSC.

Let us consider the attitude motion of the relatively small DSSC with normal distribution of the mass (without the extremely expressed inertia-mass configuration like the "gravitational dumbbell"), when the difference of the inertia moments does not exceed δ_I={1÷10} kg·m^2. Then it is possible to estimate the comparative magnitudes of the main influences (gravitational and magnetic). If we take as initial conditions the parameters of the ordinal orbital motion (including geostationary orbits) and parameters of the ordinal small magnetic SC, the estimation follows:

$$\left|\mathbf{M}_G\right| \sim 12 \cdot 10^{14} \cdot \frac{\delta_I}{R^3};\ \left|\mathbf{M}_{\boldsymbol{\theta}}\right| \sim 8 \cdot 10^{15} \cdot \frac{m}{R^3};$$

$$\left|\mathbf{M}_G\right| / \left|\mathbf{M}_{\boldsymbol{\theta}}\right| \sim \frac{\delta_I}{10 \cdot m} \sim \left\{10^{-4} \div 10^{-2}\right\}.$$

As we can see, the magnitude of the gravity gradient

torque in the considered case is less than the value of the magnetic torque by three orders (on the average) - it corresponds to the significant predominance of the magnetic torque over others torques; and in this case the results/findings [26] are applicable, including the unperturbed general solutions for the magnetic DSSC attitude motion.

So, in this research we will take into account only general influence, which corresponds to the magnetic torque. Then equations (2) take the form:

$$A\dot{p}+\left(C_2-B\right)qr+q\Delta=-Q\gamma_2;$$
$$B\dot{q}+\left(A-C_2\right)pr-p\Delta=Q\gamma_1; \quad (5)$$
$$C_2\dot{r}+\dot{\Delta}+\left(B-A\right)pq=0; \quad \dot{\Delta}=M_{\Delta}$$
$$Q=const=\pm\left|B_{orb}m\right| \quad (6)$$

We assume the following conditions:

$$A_2>B_2>C_2>A_1>C_1, \quad \Delta=\text{const}>0.$$

Also in our research we will use the Hamiltonian form of equations in the well-known Andoyer–Deprit canonical variables. The Andoyer–Deprit variables [11, 12] (l, L, I_2, I_3) are expressed through components of the system's angular momentum (Fig.2): $\mathbf{K}=\mathbf{K}\big|_{Ox_2y_2z_2}=\left[K_{x_2},K_{y_2},K_{z_2}\right]^T$

$$L=\frac{\partial T}{\partial\dot{l}}=\mathbf{K}\cdot\mathbf{k};$$
$$I_2=\frac{\partial T}{\partial\dot{\varphi}_2}=\mathbf{K}\cdot\mathbf{s}=\left|\mathbf{K}\right|=K; \quad (7)$$
$$I_3=\frac{\partial T}{\partial\dot{\varphi}_3}=\mathbf{K}\cdot\mathbf{k}'; \quad L\le I_2$$
$$K_{x_2}=Ap=\sqrt{I_2^2-L^2}\sin l;$$
$$K_{y_2}=Bq=\sqrt{I_2^2-L^2}\cos l; \quad (8)$$
$$K_{z_2}=C_2r+\Delta=L$$

The system Hamiltonian in the Andoyer–Deprit phase space has the form [e.g. 4-10]:

$$\mathcal{H}=\mathcal{H}_0+\varepsilon\mathcal{H}_1; \quad \mathcal{H}_0=T+P;$$
$$T=\frac{I_2^2-L^2}{2}\left[\frac{\sin^2 l}{A_1+A_2}+\frac{\cos^2 l}{A_1+B_2}\right]+\frac{1}{2}\left[\frac{\Delta^2}{C_1}+\frac{\left(L-\Delta\right)^2}{C_2}\right], \quad (9)$$

where T – is the system's kinetic energy; P – is the potential energy; $\varepsilon\mathcal{H}_1$ – is the small perturbed part of the Hamiltonian. In the considered case the potential energy corresponds to the "magnetic" torque (or, as it was described in [26], to the restoring/overturning torque from the system's weight in the generalized coaxial Lagrange top) – it takes the form depending only on the nutation angle:

$$P=Q\cos\theta; \quad M_{\theta}=-\frac{\partial P}{\partial\theta}=Q\sin\theta \quad (10)$$

Repeating the main findings of the previous work [26] we underscore the full compliance (in a dynamic sense) of two mechanical models (Fig.2): the magnetic/magnetized DSSC (Fig.2-a) and the coaxial Lagrange top (the heavy coaxial top) motion (Fig.2-b). Here we have to note that the Lagrange top in the classical formulation [1-4] describes the angular motion of the heavy body about fixed point O when the gravity force **W** (the system weight) is applied in the point O_W on the general longitudinal axis Oz_2. In our consideration the both models (the magnetic DSSC and the heavy coaxial top) are reduced to the interconnected common case at the corresponding conversion of the torque's magnitude (depending on proper signs of the values):

$$Q=\pm\left|B_{orb}m\right|=\mp\left|W\cdot OO_W\right|; \quad (11)$$

Therefore, the paper results and conclusions will be applicable to the both tasks (the magnetic/magnetized DSSC, and generalized heavy coaxial Lagrange top).

3. Heteroclinic analytical solutions for the angular momentum components

Let us consider the angular motion of the magnetic/magnetized DSSC in the "cylindrical precession" regime in the case when the vector of the angular momentum **K** is directed strongly along the inertial ("fixed") axis OZ $\left(\mathbf{K}=K\,\mathbf{k}'\right)$ coinciding with the vector of the external magnetic field $\left(\mathbf{B_{orb}}\right)$. In this case the system angular momentum **K** is the constant vector, and then we can rewrite the expressions (4) for the directional cosines, and the canonical Andoyer–Deprit momentums (7) as follows:

$$\begin{cases}\gamma_1=\dfrac{K_{x_2}}{K}=\dfrac{Ap}{K},\\ \gamma_2=\dfrac{K_{y_2}}{K}=\dfrac{Bq}{K},\\ \gamma_3=\dfrac{K_{z_2}}{K}=\dfrac{C_2r+\Delta}{K}\end{cases} \quad (12)$$

$$\begin{cases}L=K_{z_2}=C_2r+\Delta;\\ I_2=I_3=K=\text{const};\\ \cos\theta=\dfrac{K_{z_2}}{K}=\dfrac{C_2r+\Delta}{K}=\dfrac{L}{I_2},\end{cases} \quad (13)$$

Using (12) it is possible to rewrite the

components of the magnetic torque:

$$\mathbf{M_0}\big|_{Ox_2y_2z_2} = \left[\frac{-QK_{y_2}}{K}, \frac{QK_{x_2}}{K}, 0\right]^T = \\ = \left[\frac{-QBq}{K}, \frac{QAp}{K}, 0\right]^T \quad (14)$$

Finally the dynamical equations (5) take the form

$$A\dot{p} + (C_2 - B)qr + q\Delta = -QBq/K; \\ B\dot{q} + (A - C_2)pr - p\Delta = QAp/K; \quad (15) \\ C_2\dot{r} + \dot{\Delta} + (B - A)pq = 0; \quad \dot{\Delta} = M_\Delta$$

Also, taking into account (13), we can write the final shape of the Hamiltonian

$$\mathcal{H} = \frac{I_2^2 - L^2}{2}\left[\frac{\sin^2 l}{A_1 + A_2} + \frac{\cos^2 l}{A_1 + B_2}\right] + \\ + \frac{1}{2}\left[\frac{\Delta^2}{C_1} + \frac{(L-\Delta)^2}{C_2}\right] + Q\frac{L}{I_2} \quad (16)$$

The Hamiltonian (16) does not depend on the canonical coordinates φ_2, φ_3, then impulses I_2, I_3 are constant; and the dynamical system is reduced to one degree of freedom $\{l, L\}$:

$$\begin{cases} \dot{L} = f_L(l, L) + \varepsilon g_L; \\ \dot{l} = f_l(l, L) + \varepsilon g_l; \end{cases} \\ f_L = -\frac{\partial \mathcal{H}_0}{\partial l}; \quad f_l = \frac{\partial \mathcal{H}_0}{\partial L}; \quad (17) \\ g_L = -\frac{\partial \mathcal{H}_1}{\partial l}; \quad g_l = \frac{\partial \mathcal{H}_1}{\partial L};$$

Let us obtain the analytical solution for the heteroclinic orbits/polhodes $(S_1 \to S_2)$ in the phase space of the angular velocity components {*p*, *q*, *r*, *σ*} (Fig.3) by full analogy with the previous results [10].

Theorem. *Assume the absence of the coaxial bodies interaction* $(M_\Delta = 0)$. *Then we have the following heteroclinic solutions* $\{\bar{p}(t), \bar{q}(t), \bar{r}(t)\}$ *for the system* (15)*:*

$$\begin{cases} \bar{p}(t) = \pm\sqrt{\frac{C_2(B-C_2)}{A(A-B)}}\, y(t); \\ \bar{q}(t) = \pm\sqrt{s^2 - k^2\left(y(t) + \Delta\beta + E\alpha\right)^2}; \\ \bar{r}(t) = y(t) + \frac{\Delta - EB}{B - C_2}; \\ \bar{\sigma}(t) = \frac{\Delta}{C_1} - \bar{r}(t); \end{cases} \quad (18)$$

where

$$y(t) = \frac{4a_0 E\left(y_0^{\pm}\right)\exp\left(\mp\frac{\tilde{M}\sqrt{a_0}}{k^2}t\right)}{\left[E\left(y_0^{\pm}\right)\exp\left(\mp\frac{\tilde{M}t\sqrt{a_0}}{k^2}\right) - a_1\right]^2 - 4a_2a_0},$$

with the set of constants:

$\Delta = \text{const} > 0;$

$a_2 = -k^2;$

$a_1 = -2(\Delta\beta + E\alpha)k^2;$

$a_0 = s^2 - k^2(\Delta\beta + E\alpha)^2;$

$y_0^{\pm} = \pm\frac{s}{k} - (\Delta\beta + E\alpha);$

$\alpha = \frac{A}{A - C_2} - \frac{B}{B - C_2};$

$\beta = \frac{1}{B - C_2} - \frac{1}{A - C_2}$

$s^2 = \frac{\tilde{H}}{B(A-B)}; \quad k^2 = \frac{C_2(A-C_2)}{B(A-B)};$

$\tilde{H} = 2\tilde{T}(A - \tilde{D}) + \frac{C_2}{A - C_2}(\Delta - EA)^2 -$

$-\left[\left(\frac{A}{C_1} - 1\right)\Delta^2 + 2EA\Delta\right];$

$\tilde{T} = T_0 - Q\frac{C_2 r_0 + \Delta}{K} = \text{const};$

$2T_0 = Ap_0^2 + Bq_0^2 + C_2 r_0^2 + \frac{\Delta^2}{C_1};$

$\tilde{D} = B + \frac{1}{2\tilde{T}}\left(\frac{C_2}{B - C_2}(\Delta - EB)^2 -\right.$

$\left.-\left[\left(\frac{B}{C_1} - 1\right)\Delta^2 + 2EB\Delta\right]\right)$

$E = -\frac{Q}{K}; \quad \tilde{M} = \frac{(A - C_2)}{B}\sqrt{\frac{C_2(B-C_2)}{A(A-B)}}.$

The proof.

Let us prove the theorem directly following to the algorithm which was used in the paper [10].

We will use the polhodes geometry [1-3]. The polhode is the fourth-order curve in 3D-space (Fig.3) corresponding to the intersection of a kinetic energy ellipsoid and an angular momentum ellipsoid, which are defined with the help of the expressions for the dynamical theorems/laws of the changing of the kinetic energy and the angular momentum:

$$Ap^2 + Bq^2 + C_2 r^2 + \frac{\Delta^2}{C_1} - 2T_0 = \quad (19)$$
$$= 2P(\theta) - 2P(\theta_0)$$

$$A^2 p^2 + B^2 q^2 + \left[C_2 r + \Delta\right]^2 = K^2 \quad (20)$$

With the help of (10) and (13) we can write the expressions (19) and (20) in the form

$$Ap^2 + Bq^2 + C_2 r^2 + \frac{\Delta^2}{C_1} + 2E\left(C_2 r + \Delta\right) = 2\tilde{T} \quad (21)$$

$$A^2 p^2 + B^2 q^2 + \left[C_2 r + \Delta\right]^2 = K^2 = 2D\tilde{T} \quad (22)$$

with the following constants

$$2T_0 = Ap_0^2 + Bq_0^2 + C_2 r_0^2 + \frac{\Delta^2}{C_1};$$
$$\tilde{T} = T_0 - Q\frac{C_2 r_0 + \Delta}{K} = \text{const}; \quad (23)$$
$$E = -\frac{Q}{K}; \quad D = \frac{K^2}{2\tilde{T}}$$

Based on a combination of the expressions (21) and (22) (using the multiplication of (21) by A with the subsequent subtraction of (22)) we obtain:

$$B(A-B)q^2 +$$
$$+A\left(C_2 r^2 + \frac{\Delta^2}{C_1} + 2E\left[C_2 r + \Delta\right]\right) - \quad (24)$$
$$-\left[C_2 r + \Delta\right]^2 = 2\tilde{T}(A-D)$$

Analogically, after the multiplication of (21) by B with the subsequent subtraction of (22) we receive

$$A(B-A)p^2 +$$
$$+B\left(C_2 r^2 + \frac{\Delta^2}{C_1} + 2E\left[C_2 r + \Delta\right]\right) - \quad (25)$$
$$-\left[C_2 r + \Delta\right]^2 = 2\tilde{T}(B-D)$$

The separation of a perfect square in (25) gives the equation for hyperbolae (corresponding curves are depicted at the coordinate plane Opr – Fig.3)

$$-A(A-B)p^2 +$$
$$+C_2(B-C_2)\left[r - \frac{\Delta - EB}{B-C_2}\right]^2 = F \quad (26)$$

where

$$F = 2\tilde{T}(B-D) +$$
$$+\frac{C_2}{B-C_2}(\Delta - EB)^2 - \quad (27)$$
$$-\left[\left(\frac{B}{C_1} - 1\right)\Delta^2 + 2EB\Delta\right]$$

Now we can use the shifted coordinate axes $\tilde{O}\tilde{p}\tilde{r}$ (Fig.3) and the scalable component of the angular velocity

$$\tilde{r} = r - \frac{\Delta - EB}{B - C_2} \quad (28)$$

As a result we write in the plane $\tilde{O}\tilde{p}\tilde{r}$ canonical form of the hyperbolas equation

$$-A(A-B)p^2 + C_2(B-C_2)\tilde{r}^2 = F \quad (29)$$

The asymptotes of the hyperbolas correspond to the value F=0 and, therefore, to the following straight line equation:

$$\sqrt{A(A-B)}\,p = \pm\sqrt{C_2(B-C_2)}\,\tilde{r} \quad (30)$$

So, the equation

$$F = 0 \quad (31)$$

defines the initial conditions of the motion realization along hyperbolas' asymptotes. We can consider the equation (31) as an equation on value D

$$F = 0 \;\Rightarrow\; D = \tilde{D}$$
$$\tilde{D} = B + \frac{1}{2\tilde{T}}\left(\frac{C_2}{B-C_2}(\Delta - EB)^2 - \right. \quad (32)$$
$$\left. -\left[\left(\frac{B}{C_1} - 1\right)\Delta^2 + 2EB\Delta\right]\right)$$

Thereby, at the value $D = \tilde{D}$ the system realizes the motion along the hyperbolas asymptotes.

Let us choose the trivial initial condition for the component $q(t=0) = q_0 = 0$ which is equivalent to taking as a time-datum the time-moment when the q-component takes on the zero-value. Then the equation (31) can be rewritten in the form of the quadratic equation for the initial value r_0 (at arbitrary values p_0 and Δ)

$$B\left[Ap_0^2 + C_2 r_0^2 + \frac{\Delta^2}{C_1} - Q\frac{C_2 r_0 + \Delta}{2K}\right] - K^2 +$$
$$+\frac{C_2}{B-C_2}(\Delta - EB)^2 - \quad (33)$$
$$-\left[\left(\frac{B}{C_1} - 1\right)\Delta^2 + 2EB\Delta\right] = 0$$

So, we can find the value r_0 as the root of the eq. (33), which guarantees the equality $D = \tilde{D}$ and the motion along the hyperbolas asymptotes

$$r_0 = r_0^{(1,2)} = f(p_0, \Delta) \quad (34)$$

From the eq. (24), taking into account a perfect square, the expression follows

$$B(A-B)q^2 + \\ +C_2(A-C_2)\left[r-\frac{\Delta-EA}{A-C_2}\right]^2 = H \quad (35)$$

$$H = 2\tilde{T}(A-D)+ \\ +\frac{C_2}{A-C_2}(\Delta-EA)^2 - \quad (36) \\ -\left[\left(\frac{A}{C_1}-1\right)\Delta^2+2EA\Delta\right]$$

From (35) we obtain

$$r-\frac{\Delta-EA}{A-C_2} = \pm\sqrt{\frac{H-B(A-B)q^2}{C_2(A-C_2)}} \quad (37)$$

Also we can consider (35) as the canonical equation for ellipses on the coordinate plane *Oqr* (Fig.3). The substitution of the equality $D=\tilde{D}$ into the expression (35) gives us the equation for the "large ellipses" (black curves S_1S_2 at the Fig.3), which correspond to the projections of the heteroclinic separatrices-polhodes:

$$B(A-B)q^2 + C_2(A-C_2)\tilde{\tilde{r}}^2 = \tilde{H} \quad (38)$$

where we use the following parameter

$$\tilde{H} = 2\tilde{T}(A-\tilde{D})+\frac{C_2}{A-C_2}(\Delta-EA)^2 - \\ -\left[\left(\frac{A}{C_1}-1\right)\Delta^2+2EA\Delta\right]$$

and a scalable component of the angular velocity

$$\tilde{\tilde{r}} = r-\frac{\Delta-EA}{A-C_2} \quad (39)$$

From the equation (30) we obtain

$$p = \pm\tilde{r}\sqrt{\frac{C_2(B-C_2)}{A(A-B)}}$$

also the following form is useful

$$p = \pm\sqrt{\frac{C_2(B-C_2)}{A(A-B)}}\left[\tilde{\tilde{r}}-\Delta\beta-E\alpha\right] \quad (40)$$

It is needed to note, that the ellipse's canonical equation (38) is written in the shifted frame $\tilde{\tilde{O}}\tilde{\tilde{q}}\tilde{\tilde{r}}$.

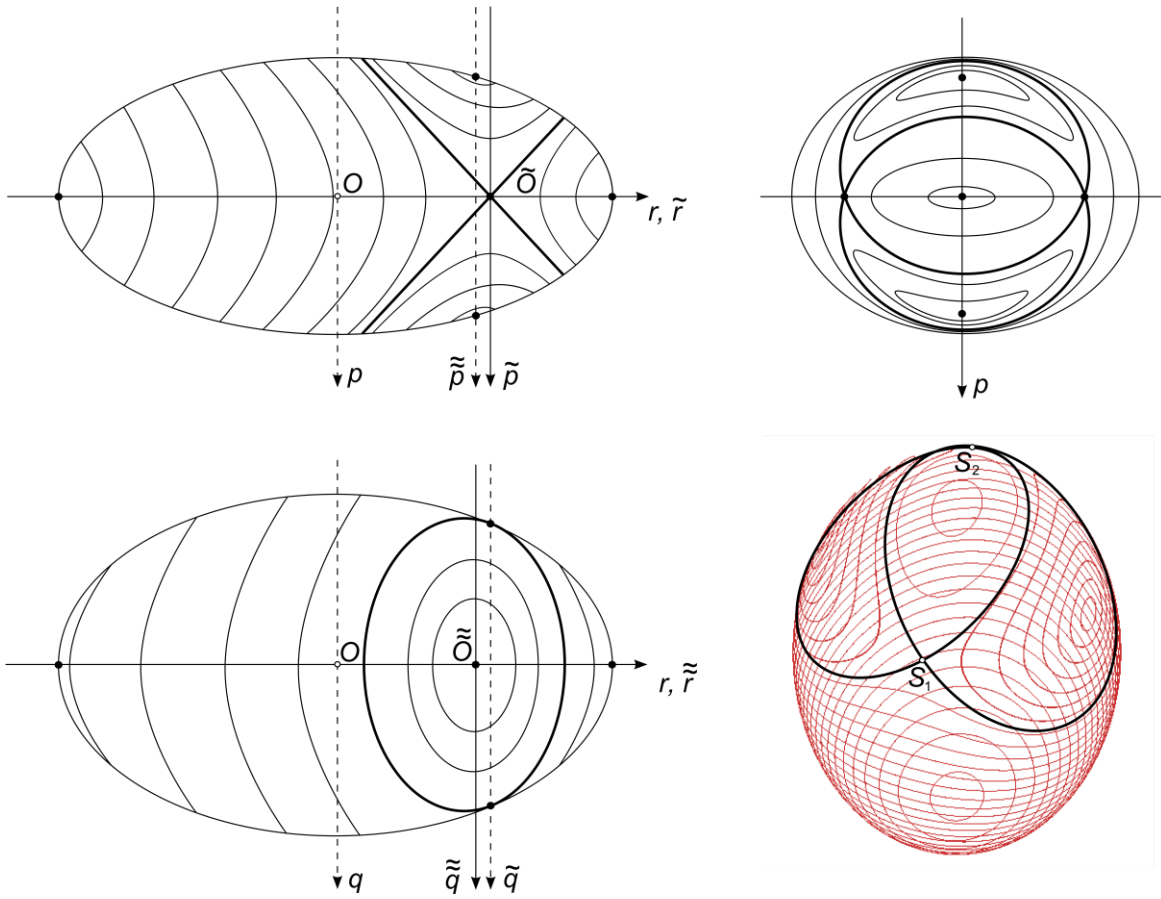

Fig.3 *The polhodes in the phase space of the angular velocity components*

From (38) the expression follow

$$\tilde{\tilde{r}}^2 = \frac{s^2 - q^2}{k^2} \tag{41}$$

where

$$s^2 = \frac{\tilde{H}}{B(A-B)} = \text{const};\ \ k^2 = \frac{C_2(A-C_2)}{B(A-B)} = \text{const}$$

The second equation (15) can be written as follows

$$B\dot{q} + (A-C_2)\left(r - \frac{\Delta - EA}{A-C_2}\right)p = 0 \tag{42}$$

With the help of (41) and (40) the last equation is reduced to the form

$$B\dot{q} \pm (A-C_2)\sqrt{\frac{s^2-q^2}{k^2}} \times \\ \times \sqrt{\frac{C_2(B-C_2)}{A(A-B)}}\left[\pm\sqrt{\frac{s^2-q^2}{k^2}} - \Delta\beta - E\alpha\right] = 0 \tag{43}$$

The differential equation (43) contains a possible quaternary signs alternation, corresponded to the four heteroclinic orbits "saddle-to-saddle" $(S_1 \to S_2)$. These four orbits form the "large ellipses".

We can make the change of variables

$$x = \sqrt{\frac{s^2-q^2}{k^2}} \tag{44}$$

From (44) the expressions follow

$$q = \pm\sqrt{s^2 - k^2x^2}; \qquad dq = \frac{\mp k^2 x dx}{\sqrt{s^2-k^2x^2}}$$

Then the equation (43) is rewritten in a differential form

$$\frac{k^2 dx}{\left[\pm x - \Delta\beta - E\alpha\right]\sqrt{s^2-k^2x^2}} = \pm\tilde{M}dt \\ \tilde{M} = \frac{(A-C_2)}{B}\sqrt{\frac{C_2(B-C_2)}{A(A-B)}} \tag{45}$$

The equation (45) includes two cases of signs of the *x*-variable. In the both cases we make corresponding substitutions

$$1).\ \left|\begin{array}{l} \dfrac{k^2 dx}{\left[x - \Delta\beta - E\alpha\right]\sqrt{s^2-k^2x^2}} = \pm\tilde{M}dt \\ y = x - \Delta\beta - E\alpha \\ x = y + \Delta\beta + E\alpha;\ \ dx = dy \\ y_0 = x_0 - \Delta\beta - E\alpha \\ \dfrac{k^2 dy}{y\sqrt{s^2-k^2x^2}} = \pm\tilde{M}dt \end{array}\right. \tag{46}$$

$$2).\ \left|\begin{array}{l} \dfrac{k^2 dx}{\left[-x - \Delta\beta - E\alpha\right]\sqrt{s^2-k^2x^2}} = \pm\tilde{M}dt \\ y = -x - \Delta\beta - E\alpha \\ x = -y - \Delta\beta - E\alpha;\ \ dx = -dy \\ y_0 = -x_0 - \Delta\beta - E\alpha \\ \dfrac{-k^2 dy}{y\sqrt{s^2-k^2x^2}} = \pm\tilde{M}dt \end{array}\right.$$

As we can see from the expressions (46), the both cases give the interconnected equation again

$$\frac{k^2 dy}{y\sqrt{s^2-k^2x^2}} = \pm\tilde{M}dt \tag{47}$$

Taking into account the twoness of the initial condition $(y_0 = \pm x_0 - \Delta\beta - E\alpha)$ from (47) the integral expression follows

$$\int_{y_0}^{y} \frac{dy}{y\sqrt{s^2 - k^2\left(y^2 + 2\left[\Delta\beta + E\alpha\right]y + \left[\Delta\beta + E\alpha\right]^2\right)}} = \\ = \frac{\pm\tilde{M}t}{k^2}; \tag{48}$$

$$y_0 = y_0^{\pm} = \pm x_0 - \Delta\beta - E\alpha;\ \ x_0 = \frac{s}{k}$$

The expression (48) reduces to the standard integral

$$\int_{y_0}^{y} \frac{dy}{y\sqrt{a_2y^2 + a_1y + a_0}} = \mathbb{F}(y) - \mathbb{F}(y_0^{\pm}); \\ a_2 = -k^2;\ \ a_1 = -2\left[\Delta\beta + E\alpha\right]k^2; \\ a_0 = s^2 - k^2\left[\Delta\beta + E\alpha\right]^2 \tag{49}$$

where the antiderivative $\mathbb{F}(y)$ has the following standard shape

$$\mathbb{F}(z) = \frac{-1}{\sqrt{a_0}}\ln E(z);\quad a_0 > 0; \\ E(z) = \frac{2a_0 + a_1 z + 2\sqrt{a_0}\sqrt{a_2z^2 + a_1z + a_0}}{z}$$

From (49) we get the solution for the equation (47)

$$E(y(t)) = E(y_0^{\pm})\exp\left(\mp\frac{M\sqrt{a_0}}{k^2}t\right) \tag{50}$$

After transformations the exact explicit analytical solution for the time-series *y*(*t*) follows

$$y(t) = \frac{4a_0E(y_0^{\pm})\exp\left(\mp\dfrac{M\sqrt{a_0}}{k^2}t\right)}{\left[E(y_0^{\pm})\exp\left(\mp\dfrac{Mt\sqrt{a_0}}{k^2}\right) - a_1\right]^2 - 4a_2a_0} \tag{51}$$

It is needed to note, that the quadrature (49) is quite frequent for heteroclinic solutions in rigid body dynamics [e.g. 7-10].

Making back substitutions we get the exact explicit analytical heteroclinic parametrized solutions for all components of the angular velocity $\{\bar{p}(t),\bar{q}(t),\bar{r}(t)\}$:

$$\begin{cases} \bar{p}(t)=\pm\sqrt{\dfrac{C_2(B-C_2)}{A(A-B)}}\,y(t); \\ \bar{q}(t)=\pm\sqrt{s^2-k^2\left(y(t)+\Delta\beta+E\alpha\right)^2}; \\ \bar{r}(t)=y(t)+\dfrac{\Delta-EB}{B-C_2}; \\ \bar{\sigma}(t)=\dfrac{\Delta}{C_1}-\bar{r}(t) \end{cases} \tag{52}$$

The *theorem* is completely proved.

We have to additionally underline, that the heteroclinic solutions also can be obtained using functional transformations of the general solutions [26] at the condition of the hyperbolic singularity of the elliptic integrals and functions (the elliptic modulus k=1), when the elliptic functions express in terms of hyperbolic functions. However, the considered way (based on the theorem's proof) of the heteroclinic solutions obtaining is the preferable, natural and geometrically clear technique.

Figure (Fig.4) demonstrates the validity of the solutions (52) as the comprehensive coincidence of the calculation results (by the analytical dependences - points) with the numerical integration results (lines). The upper graphs (Fig.4-a) correspond to the first root $r_0^{(1)}$ of the quadratic equation (31), and the graphs (fig.4-b) correspond to the second root $r_0^{(2)}$.

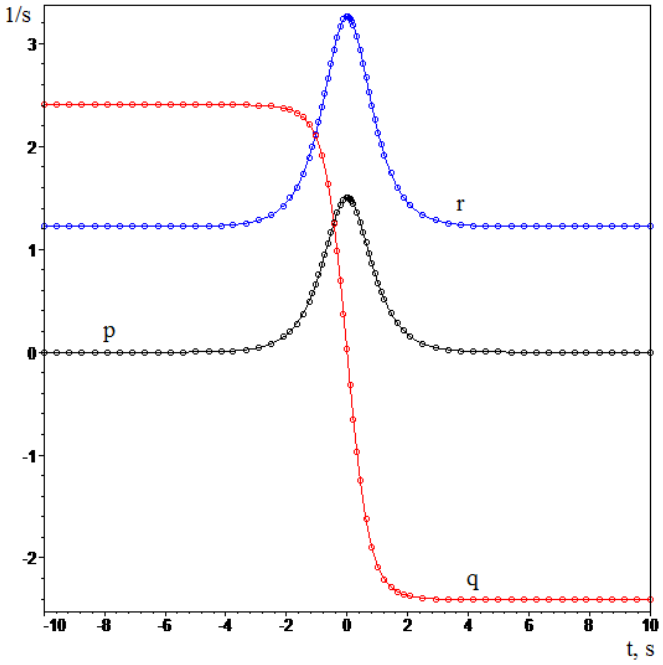

(a)

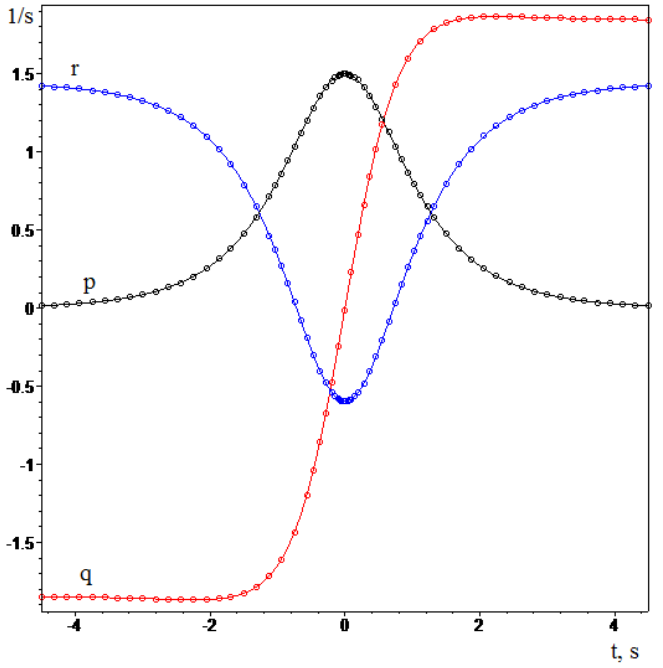

(b)

Fig.4 *The heteroclinic dependences*:

$A_2=15,\ B_2=10,\ C_2=6,\ A_1=5,\ C_1=4\ [kg\cdot m^2];$

$Q=20\ [kg\cdot m^2/s^2];\ \Delta=3\ [kg\cdot m^2/s];\ p_0=1.5[1/s]$

a). $r_0=r_0^{(1)}=3.262;\ \ \sigma_0^{(1)}=-2.512$ [1/s]

b). $r_0=r_0^{(2)}=-0.597;\ \ \sigma_0^{(2)}=1.347$ [1/s]

It is worth to note that the solutions (52) allow the easy transformation to the Andoyer–Deprit heteroclinc dependences:

$$\begin{aligned}
&\bar{L}(t) = C_2\bar{r}(t) + \Delta = C_2 y(t) + W;\\
&\bar{l}(t) = \arcsin\frac{A\bar{p}(t)}{\sqrt{I_2^2 - \bar{L}^2(t)}} =\\
&= \pm\arcsin\frac{Vy(t)}{\sqrt{I_2^2 - \left(C_2 y(t) + W\right)^2}};\\
&\bar{l}\left(\bar{L}(t)\right) = \pm\arcsin\frac{V\bar{L}(t) - W}{C_2\sqrt{I_2^2 - \bar{L}^2(t)}};
\end{aligned} \tag{53}$$

where

$$V = \sqrt{\frac{AC_2(B - C_2)}{(A - B)}} = \text{const};$$

$$W = \frac{B}{B - C_2}\left[\Delta - C_2 E\right] = \text{const}.$$

The solutions (52) and (53) generalize the well-known heteroclinic dependencies for the free rigid body and for free coaxial bodies, which were used in numerous research works, for example [7-10, 13, 23, 24].

4. The motion chaotization analysis

Let us examine some features of the system motion chaotization at the presence of the perturbation corresponding to the action of small complex variations/oscillations in the magnetic moment of the DSSC $\left(m = \bar{m} + \nu\tilde{m}(t)\right)$, or in the magnet Earth-dipole $\left(B_{orb} = \bar{B}_{orb} + \mu\tilde{B}(t)\right)$, or in the case of the variations of the both values composition. Then this complexified perturbation can be expressed by the use of the time-series of the value Q (6) in the form of the sum of the generating "unperturbed" constant part Q_0 and the small varying part $Q_1(t)$:

$$Q(t) = Q_0 + Q_1(t) = Q_0\left(1 + \varepsilon\tilde{Q}(t)\right) \tag{54}$$

$$Q_0 = \bar{B}_{orb}\bar{m}; \qquad \varepsilon\tilde{Q}(t) = \frac{Q_1(t)}{Q_0};$$

where the dimensionless small parameter ε scales the smallness of the perturbation – this parameter can be defined by standard ways, but in this research we do not focus on this aspect. Indeed, in our research we will use the shape of the varying part, which is actual practically in any case of a periodical perturbation and corresponds to the general form of the expansion in a Fourier series (taking into account N harmonic components) [21]:

$$\tilde{Q}(t) = \sum_{n=0}^{N}\left[\bar{a}_n\sin\left(n\omega_p t\right) + \bar{b}_n\cos\left(n\omega_p t\right)\right] \tag{55}$$

where T_p is the main period of the perturbation; $\omega_p = 2\pi/T_p$ - is the main frequency of perturbation, $\bar{a}_n$, $\bar{b}_n$ are the constant Fourier coefficients. At the presence of the perturbation (55) the perturbed Hamiltonian can be rewritten

$$\begin{aligned}
&\mathcal{H} = \mathcal{H}_0 + \varepsilon\mathcal{H}_1\\
&\mathcal{H}_0 = \frac{I_2^2 - L^2}{2}\left[\frac{\sin^2 l}{A_1 + A_2} + \frac{\cos^2 l}{A_1 + B_2}\right] +\\
&+\frac{1}{2}\left[\frac{\Delta^2}{C_1} + \frac{(L - \Delta)^2}{C_2}\right] + Q_0\frac{L}{I_2};\\
&\mathcal{H}_1 = Q_0\tilde{Q}(t)\frac{L}{I_2}
\end{aligned} \tag{56}$$

Then we have the following right parts (17) of the dynamical equations

$$\begin{cases}
f_L(l, L) = \left(\frac{1}{B} - \frac{1}{A}\right)\left(I_2^2 - L^2\right)\sin l\cos l;\\
f_l(l, L) = L\left[\frac{1}{C_2} - \frac{\sin^2 l}{(A_1 + A_2)} - \frac{\cos^2 l}{(A_1 + B_2)}\right] -\\
-\frac{\Delta}{C_2} + \frac{Q_0}{I_2};
\end{cases}$$

$$\begin{cases}
g_L = 0;\\
g_l = \frac{Q_0\tilde{Q}(t)}{I_2} = \eta\sum_{n=0}^{N}\left[\bar{a}_n\sin\left(n\omega_p t\right) + \bar{b}_n\cos\left(n\omega_p t\right)\right],
\end{cases}$$

where $\eta = \frac{Q_0}{I_2}$.

Then the Melnikov function in considered case takes the similar with results [29-31, 10, 23] form:

$$M(t_0) = \varepsilon\int_{-\infty}^{+\infty} f_L\left(\bar{l}(t), \bar{L}(t)\right)g_l(t + t_0)\,dt \tag{57}$$

where the $f_L\left(\bar{l}(t), \bar{L}(t)\right)$ can be directly expressed through heteroclinic dependences $\bar{p}(t), \bar{q}(t), \bar{r}(t)$ based on the expressions (8):

$$\begin{aligned}
&f_L(\bar{l}, \bar{L}) = \left(\frac{1}{B} - \frac{1}{A}\right)\left(I_2^2 - \bar{L}^2\right)\sin\bar{l}\cos\bar{l} =\\
&= \left(\frac{1}{B} - \frac{1}{A}\right)A\bar{p}(t)B\bar{q}(t)
\end{aligned}$$

Then the Melnikov function is evaluated as follows

$$M\left(t_0\right)=\varepsilon\lambda\int\limits_{-\infty}^{+\infty}A\bar{p}(t)B\bar{q}(t)\times$$

$$\times\sum_{n=0}^{N}\left[\bar{a}_n\sin n\omega_p\left(t+t_0\right)+\bar{b}_n\cos n\omega_p\left(t+t_0\right)\right]dt=$$

$$=\varepsilon\lambda\sum_{n=0}^{N}\left[J_s^{(n)}\left\{\bar{a}_n\cos n\omega_p t_0-\bar{b}_n\sin n\omega_p t_0\right\}+\right.$$

$$\left.+J_c^{(n)}\left\{\bar{a}_n\sin n\omega_p t_0+\bar{b}_n\cos n\omega_p t_0\right\}\right],$$

$$J_s^{(n)}=\int\limits_{-\infty}^{+\infty}\bar{g}\left(t\right)\sin\left(n\omega_p t\right)dt;$$

$$J_c^{(n)}=\int\limits_{-\infty}^{+\infty}\bar{g}\left(t\right)\cos\left(n\omega_p t\right)dt; \qquad (58)$$

$$\lambda=\eta\left(\frac{1}{B}-\frac{1}{A}\right)$$

$$\bar{g}\left(t\right)=AB\bar{p}(t)\bar{q}(t)=$$

$$=\pm\gamma\sqrt{s^2-k^2\left(y\left(t\right)+\Delta\beta+E\alpha\right)^2}\,y\left(t\right);$$

$$\gamma=AB\sqrt{\frac{C_2\left(B-C_2\right)}{A\left(A-B\right)}}$$

The function $\bar{g}\left(t\right)$ is the odd-function tended to zero (at $t\to\pm\infty$). Then the integrals (58) are convergent to the corresponding constants:

$$J_c^{(n)}=0;\quad J_s^{(n)}=\text{const}_n \qquad (59)$$

Finally we obtain the polyharmonic form of the Melnikov function:

$$M\left(t_0\right)=\varepsilon\lambda\sum_{n=0}^{N}J_s^{(n)}\left\{\bar{a}_n\cos\left(n\omega_p t_0\right)-\bar{b}_n\sin\left(n\omega_p t_0\right)\right\} \qquad (60)$$

Here we ought to note the possibility of the "quasiperiodic Melnikov function" building based on the S.Wiggins' methodology [30, 31] – this approach gives the same structure of the Melnikov function (60).

The polyharmonic form (60) defines the infinitude of simple zero-roots of the Melnikov function, that eventually confirms the fact of the local heteroclinic chaos initiation; the perturbed heteroclinic orbits form complicated heteroclinic nets with the corresponding production of the chaotic layer (the area of the phase-space with the dense cloud of the separate points of the Poincaré's intersection) near the heteroclinic separatrix region. This is one of the main reasons of the DSSC's complex tilting motion.

Certainly, there are the separate combinations of the Fourier coefficients which eliminate the roots of the Melnikov function – these combinations correspond to the antichaotization conditions and can be found in the special research.

5. Numerical modelling results

In the previous section we showed the fact of the heteroclinic chaotization using the Melnikov's method. Now we can give numerical illustrations of the chaotic properties based on the Poincaré sections (Fig.5), the time series, polhode 3D-curve plotting and the heteroclinic nets (Fig.6). The indicated Poincaré sections were plotted based on the "stroboscopic" condition of the main phase $\omega_p t$ repetition $\left\lfloor\left(\omega_p t \bmod 2\pi\right)=0\right\rfloor$ in the dimensionless Andoyer's-Deprit's phase space $\left\{l,\ L/I_2\right\}$.

First of all, we have to indicate the production of the chaotic layer near the heteroclinic separatrix region – it is showed as a cloud of blue points at the figures (Fig.5). Also at the figures (Fig.5) we can see the primary and secondary chaotic layers (in the regions of the primary and secondary separatrix bundles with the meander-line tori), and the "islands of regularity" – this is the phase portrait's areas corresponding to local oscillations regimes into the chaotic layer.

The heteroclinic nets were plotted as a collection of the Poincaré images and preimages (corresponding to the separated generations) of the unperturbed separatrix polhode's points.

So, as we can see, all of the standard features of the chaotic modes are realized: the Poincaré sections have the chaotic layers; the time-series of the angular velocity components are complex and oscillating with variable (irregular) amplitudes; the heteroclinic nets are tangled.

Conclusion

Heteroclinic dynamics of the magnitized DSSC was examined in the case of the "cylindrical precession". The heteroclinic analytical solutions for the polhode-separatrix in the phase space of the angular velocity components were obtained. These heteroclinic solutions are the main result of the paper, which can be applied to the investigation and modeling of chaotic properties of the magnetic/magnetized DSSC attitude dynamics in many cases of perturbations and conditions of the attitude motion.

As an example of the chaotization analysis, the case of polyharmonic perturbations was studied based on the Melnikov's methodology. Also the corresponding numerical modeling of the magnetic/magnetized DSSC attitude motion was fulfilled.

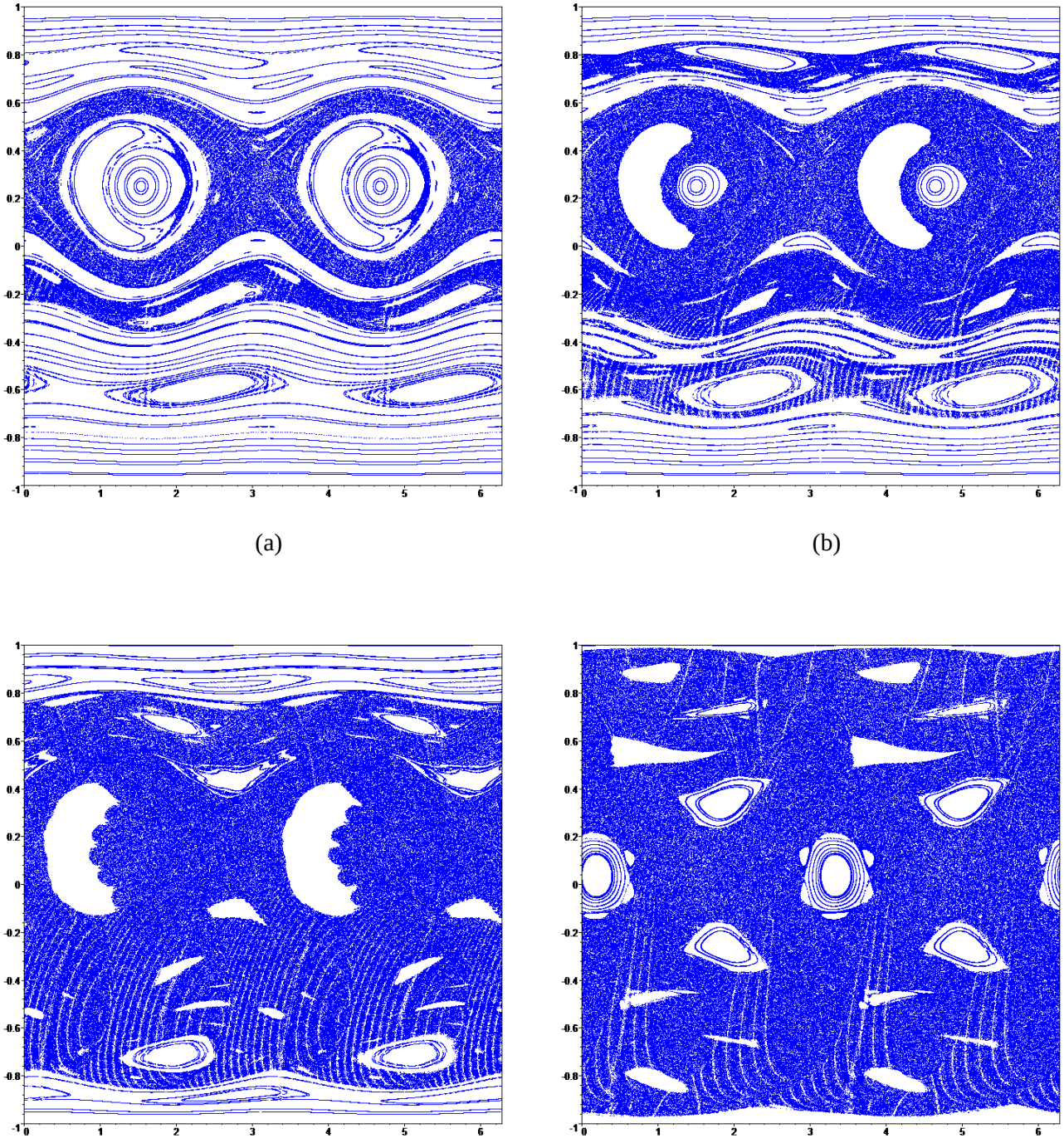

(a) (b)

(c) (d)

Fig.5. *Poincaré sections* $\left\langle \left(\omega_p t \bmod 2\pi\right)=0\right\rangle$

Numerical values of the systems parameters:

$A_2=15,\ B_2=10,\ C_2=6,\ A_1=5,\ C_1=4\ [kg\cdot m^2];$

$I_2=20,\ \Delta=5\ [kg\cdot m^2/s];\ \omega_p=0.75\ [1/s];$

$\bar{a}_1=1;\ \bar{a}_3=5;\ \bar{a}_5=20$ [dimensionless];

$Q_0\,[kg\cdot m^2/s^2]$: $a).\ Q_0=5;\ b).\ Q_0=5;\ c).\ Q_0=10;\ d).\ Q_0=15;$

ε [dimensionless]: $a).\ \varepsilon=0.04;\ b).\ \varepsilon=0.1;\ c).\ \varepsilon=0.1;\ d).\ \varepsilon=0.2$

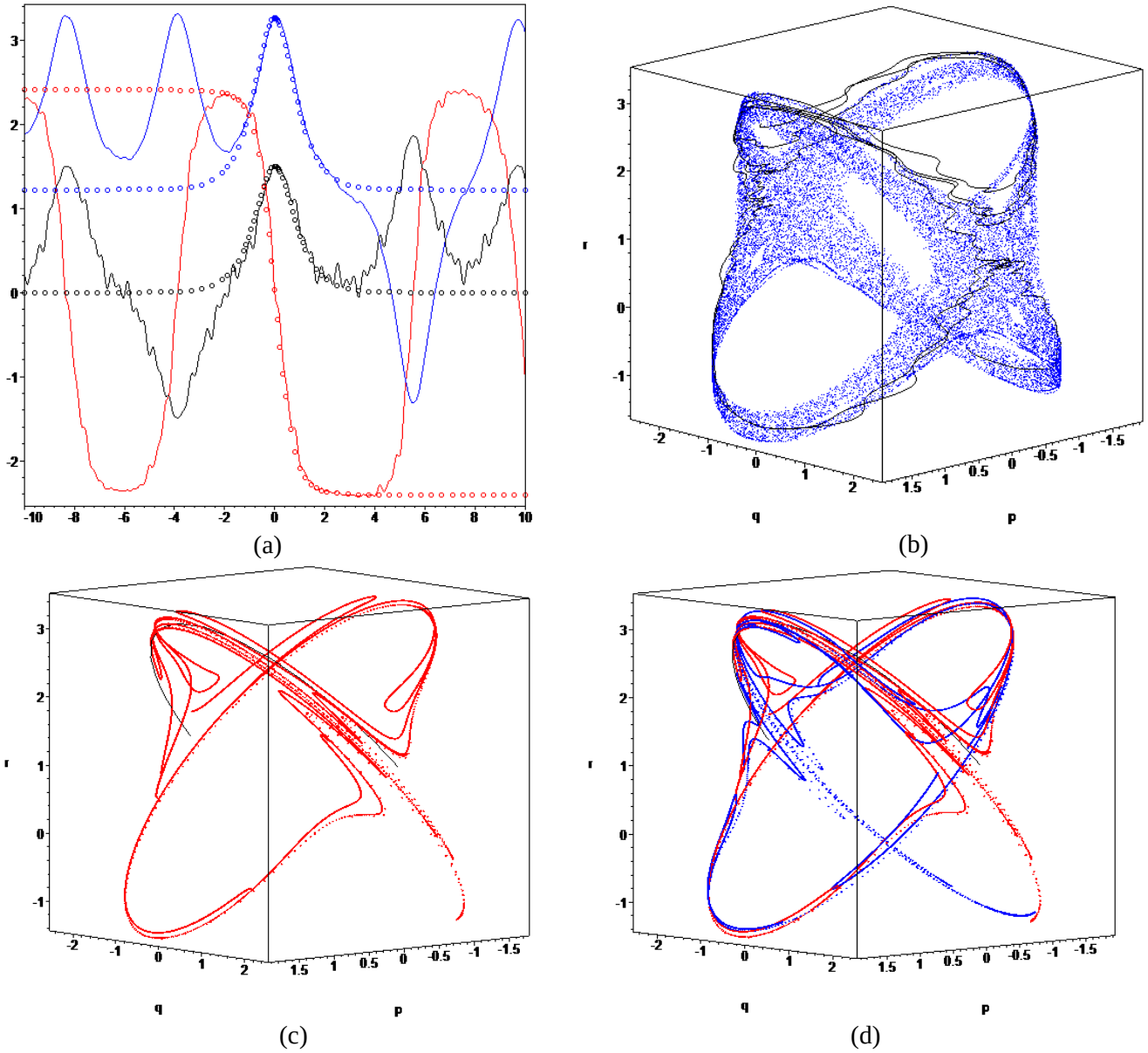

Fig.6. *The chaotic features of the heteroclinic dynamics of the magnetic/magnetized DSSC*

a) The time-history of the angular velocity components: p(t) – black; q(t) – red; r(t) – blue (points – unperturbed solutions; lines – perturbed dependences)
b) The Poincaré map of the perturbed separatrix
c) The Poincaré map as forward-images of the unperturbed separatrix (the corresponding heteroclinic net)
d) The Poincaré mapas set of preimages-images of the unperturbed separatrix (the heteroclinic net)

Numerical values of the systems parameters:

$$A_2 = 15,\ B_2 = 10,\ C_2 = 6,\ A_1 = 5,\ C_1 = 4\ [kg \cdot m^2];\quad I_2 = 20,\ \Delta = 5\ [kg \cdot m^2/s];$$

$$\omega_p = 3.75\ [1/s];\ Q_0 = 20\ [kg \cdot m^2/s^2];\quad \bar{a}_1 = 1;\ \bar{a}_3 = 5;\quad \bar{a}_5 = 20;\ \varepsilon = 0.3$$

The modeling illustrated all of the standard features of the chaotic modes: the Poincaré sections have the chaotic layers; the time-series of the angular velocity components are complex oscillating with variable (irregular) amplitudes; the heteroclinic nets are tangled.

These indicated chaotic dynamical properties in the practice of the real space-missions result in the DSSC chaotic attitude motion and in failures/anomalies of its operation; also the desired target motion of the DSSC due to this chaos phenomenon is inevitably involved in the chaotic regime, and, therefore, the stabilized regime of the magnetic/magnetized DSSC "cylindrical precession" can be lost.

The paper results are also applicable to the task of the generalized heavy coaxial Lagrange top; and, on the contrary, in the case when the magnetic moment of the DSSC is equal to zero, the investigation results are directly reduced to the Euler coaxial top [5-10].

Acknowledgment

This work was partially supported by the Ministry education and science of the Russian Federation

- in the framework of the implementation of the Program of increasing the competitiveness of SSAU among the world's leading scientific and educational centers for 2013-2020 years;
- in the framework of the State Assignments to higher education institutions and research organizations in the field of scientific activity.

References

[1] J. Wittenburg, Dynamics of Systems of Rigid Bodies. Stuttgart: Teubner, 1977.

[2] J. Wittenburg, Beitrage zur dynamik von gyrostaten, Accademia Nazional dei Lincei, Quaderno N. 227 (1975) 1–187.

[3] V.V. Golubev, Lectures on Integration of the Equations of Motion of a Rigid Body about a Fixed Point, State Publishing House of Theoretical Literature, Moscow, 1953.

[4] V.V. Kozlov, Methods of qualitative analysis in the dynamics of a rigid body, Gos. Univ., Moscow, 1980.

[5] A. Elipe, V. Lanchares, Exact solution of a triaxial gyrostat with one rotor, Celestial Mechanics and Dynamical Astronomy, Issue 1-2, Volume 101, 2008, pp 49-68.

[6] E.A. Ivin, Decomposition of variables in task about gyrostat motion. Vestnik MGU (Transactions of Moscow's University). Series: Mathematics and Mechanics. No.3 (1985) Pp. 69-72.

[7] V.S. Aslanov, Integrable cases in the dynamics of axial gyrostats and adiabatic invariants, Nonlinear Dynamics, Volume 68, Numbers 1-2 (2012) 259-273.

[8] V.S. Aslanov, A.V. Doroshin, Chaotic dynamics of an unbalanced gyrostat. Journal of Applied Mathematics and Mechanics, Volume 74, Issue 5 (2010) 525-535.

[9] A.V. Doroshin, Exact solutions for angular motion of coaxial bodies and attitude dynamics of gyrostat-satellites, International Journal of Non-linear Mechanics 50 (2013) 68-74.

[10] A.V. Doroshin, Heteroclinic dynamics and attitude motion chaotization of coaxial bodies and dual-spin spacecraft, Communications in Nonlinear Science and Numerical Simulation, Volume 17, Issue 3 (2012) 1460–1474.

[11] H. Andoyer, Cours de Mecanique Celeste, Paris: Gauthier-Villars, 1924.

[12] A. Deprit, A free rotation of a rigid body studied in the phase plane, American Journal of Physics 35 (1967) 425 – 428.

[13] P. J. Holmes, J. E. Marsden, Horseshoes and Arnold diffusion for Hamiltonian systems on Lie groups, Indiana Univ. Math. J. 32 (1983) 283-309.

[14] C.D. Hall, R.H. Rand, Spinup Dynamics of Axial Dual-Spin Spacecraft, Journal of Guidance, Control, and Dynamics, Vol. 17, No. 1 (1994) 30–37.

[15] C.D. Hall, Momentum Transfer Dynamics of a Gyrostat with a Discrete Damper, Journal of Guidance, Control, and Dynamics, Vol. 20, No. 6 (1997) 1072-1075.

[16] A.I. Neishtadt, M.L. Pivovarov, Separatrix crossing in the dynamics of a dual-spin satellite. Journal of Applied Mathematics and Mechanics, Volume 64, Issue 5, 2000, Pages 709-714.

[17] A.V. Doroshin, Evolution of the precessional motion of unbalanced gyrostats of variable structure. Journal of Applied Mathematics and Mechanics, Volume 72, Issue 3, October 2008,

Pages 259-269.

[18] A.V. Doroshin, Synthesis of attitude motion of variable mass coaxial bodies, WSEAS Transactions on Systems and Control, Issue 1, Volume 3 (2008) 50-61.

[19] A.V. Doroshin, Analysis of attitude motion evolutions of variable mass gyrostats and coaxial rigid bodies system, International Journal of Non-Linear Mechanics, Volume 45, Issue 2 (2010) 193–205.

[20] A.V. Doroshin, Modeling of chaotic motion of gyrostats in resistant environment on the base of dynamical systems with strange attractors. Communications in Nonlinear Science and Numerical Simulation, Volume 16, Issue 8 (2011) 3188–3202.

[21] A.V. Doroshin, Chaos and its avoidance in spinup dynamics of an axial dual-spin spacecraft. Acta Astronautica, Volume 94, Issue 2, February 2014, Pages 563-576.

[22] M. Iñarrea, V. Lanchares, Chaos in the reorientation process of a dual-spin spacecraft with time-dependent moments of inertia, Int. J. Bifurcation and Chaos. 10 (2000) 997-1018.

[23] A.V. Doroshin, M.M. Krikunov, Attitude dynamics of a spacecraft with variable structure at presence of harmonic perturbations, Applied Mathematical Modelling, Volume 38, Issues 7–8 (2014) 2073-2089

[24] Jinlu Kuang, Soonhie Tan, Kandiah Arichandran, A.Y.T. Leung, Chaotic dynamics of an asymmetrical gyrostat, International Journal of Non-Linear Mechanics, Volume 36, Issue 8 (2001) 1213-1233.

[25] Awad El-Gohary, Chaos and optimal control of steady-state rotation of a satellite-gyrostat on a circular orbit, Chaos, Solitons & Fractals, Volume 42, Issue (2009) 2842-2851.

[26] A.V. Doroshin, Exact Solutions in Attitude Dynamics of a Magnetic Dual-Spin Spacecraft and a Generalization of the Lagrange Top, WSEAS Transactions on Systems, Issue 10, Volume 12 (2013) 471-482.

[27] A. Guran, Chaotic motion of a Kelvin type gyrostat in a circular orbit, Acta Mech. 98 (1993) 51–61.

[28] X. Tong, B. Tabarrok, F. P. J. Rimrott, Chaotic motion of an asymmetric gyrostat in the gravitational field, Int. J. Non-Linear Mech. 30 (1995) 191-203.

[29] V.K. Melnikov, On the stability of the centre for time-periodic perturbations, Trans. Moscow Math. Soc. No.12 (1963) 1-57.

[30] S. Wiggins, Chaotic Transport in Dynamical System. Springer-Verlag. 1992.

[31] A.V. Doroshin, Homoclinic solutions and motion chaotization in attitude dynamics of a multi-spin spacecraft, Communications in Nonlinear Science and Numerical Simulation, Vol. 19, Issue 7 (2014) 2528-2552.

[32] M. Iñarrea, Chaos and its control in the pitch motion of an asymmetric magnetic spacecraft in polar elliptic orbit, Chaos, Solitons & Fractals,Volume 40, Issue 4, 30 May 2009, Pages 1637-1652.

[33] M. Iñarrea, Chaotic pitch motion of a magnetic sspacecraft with viscous drag in an elliptical polar orbit, Internatioanl Journal of Bifurcation and Chaos, Vol.21, No.7 (2011) 1959-1975.

[34] V.A. Bushenkov, M. Yu. Ovchinnikov, G.V. Smirnov, Attitude stabilization of a satellite by magnetic coils, Acta Astronautica, Volume 50, Issue 12 (2002) 721-728

[35] M.Yu. Ovchinnikov, D.S. Roldugin, V.I. Penkov, Asymptotic study of a complete magnetic attitude control cycle providing a single-axis orientation, Acta Astronautica 77 (2012) 48–60

[36] M.Yu. Ovchinnikov, A.A. Ilyin, N.V. Kupriynova, V.I. Penkov, A.S. Selivanov, Attitude dynamics of the first Russian nanosatellite TNS-0, Acta Astronautica, Volume 61, Issues 1–6, June–August 2007, Pages 277-285

[37] Yan-Zhu Liua, Hong-Jie Yu, Li-Qun Chen, Chaotic attitude motion and its control of spacecraft in elliptic orbit and geomagnetic field, Acta Astronautica 55 (2004) 487 – 494.

[38] Li-Qun Chen, Yan-Zhu Liu, Chaotic attitude motion of a magnetic rigid spacecraft and its control, International Journal of Non-Linear Mechanics 37 (2002) 493–504.

[39] Li-Qun Chen, Yan-Zhu Liu, Gong Cheng, Chaotic attitude motion of a magnetic rigid spacecraft in a circular orbit near the equatorial plane, Journal of the Franklin Institute 339 (2002) 121–128.

[40] M. Lovera, A. Astolfi, Global Magnetic Attitude Control of Spacecraft in the Presence of Gravity Gradient, IEEE Ttansactions On

Aerospace And Electronic Systems, Vol. 42, No. 3 (2006) 796-805.

[41] M. Lovera, A. Astolfi, Spacecraft attitude control using magnetic actuators, Automatica 40 (2004) 1405 – 1414.

[42] Enrico Silani, Marco Lovera, Magnetic spacecraft attitude control: a survey and some new results, Control Engineering Practice 13 (2005) 357–371.

[43] Filippo Neri, Traffic packet based intrusion detection: decision trees and generic based learning evaluation. WSEAS Transactions on Computers, WSEAS Press (Wisconsin, USA), issue 9, vol. 4, 2005, pp. 1017-1024.

[44] Filippo Neri, Software agents as a versatile simulation tool to model complex systems. WSEAS Transactions on Information Science and Applications, WSEAS Press (Wisconsin, USA), issue 5, vol. 7, 2010, pp. 609-618.

[45] L. Nechak, S. Berger, E. Aubry, Robust Analysis of Uncertain Dynamic Systems: Combination of the Centre Manifold and Polynomial Chaos theories, WSEAS Transactions on Systems, Issue 4, Volume 9, April 2010, pp.386-395.

[46] N. Jabli, H. Khammari, M. F. Mimouni, R. Dhifaoui, Bifurcation and chaos phenomena appearing in induction motor under variation of PI controller parameters, WSEAS Transactions on Systems, Issue 7, Volume 9, July 2010, pp.784-793.

[47] S. Staines A., Neri F. (2014). "A Matrix Transition Oriented Net for Modeling Distributed Complex Computer and Communication Systems". WSEAS Transactions on Systems, 13, WSEAS Press (Athens, Greece), 12-22.

[48] M. Camilleri, F. Neri, M. Papoutsidakis (2014), "An Algorithmic Approach to Parameter Selection in Machine Learning using Meta-Optimization Techniques". WSEAS Transactions on Systems,13, WSEAS Press (Athens, Greece), 202-213.

[49] M. Papoutsidakis, D. Piromalis, F. Neri, M. Camilleri (2014), "Intelligent Algorithms Based on Data Processing for Modular Robotic Vehicles Control". WSEAS Transactions on Systems, 13, WSEAS Press (Athens, Greece), 242-251.